

X-ray spectral variability of low ionization nuclear emission line regions (LINERs)

L. Hernández-García¹, O. González-Martín^{2,3,4}, J. Masegosa¹, and I. Márquez.¹

¹ Instituto de Astrofísica de Andalucía, CSIC, Glorieta de la Astronomía, s/n, 18008 Granada, Spain

² Centro de Radioastronomía y Astrofísica (CRyA-UNAM), 3-72 (Xangari), 8701, Morelia, Mexico

³ Instituto de Astrofísica de Canarias (IAC), C/ Vía Lactea, s/n, 38205 La Laguna, Tenerife, Spain

⁴ Departamento de Astrofísica, Universidad de La Laguna (ULL), 38205 La Laguna, Tenerife, Spain

Abstract

Although variability is a general property of AGN, and in LINERs variations in timescales of months/years have been found for some objects, it is not clear how these changes occur. The main purpose of this work is to investigate the X-ray variability in LINERs, including the main driver of such variations. We use the 18 LINERs in the Palomar sample with data at different epochs available in *Chandra* and/or *XMM-Newton* archives. All the spectra for the same object are simultaneously fitted to study long term variations. The nature of the variability pattern was studied allowing the different parameters to vary during the spectral fit. Whenever possible, short term variations and UV variability are studied. Short term variations are not found at X-rays. Taking into account the data at X-rays (seven out of 12 objects) and UV (five out of six), ten out of 13 LINERs show long term variations. The main driver of the X-ray variations is related to changes in the nuclear power, while changes on absorptions are found only in one case. According to their BH masses, accretion rates and variability timescales, LINERs behave as more powerful AGN at X-rays. However, we conclude that a different accretion mechanism (compared to more powerful AGN) may be present, based on the anticorrelation between Γ and the Eddington ratio.

1 Introduction

The unified model of active galactic nuclei (AGN), which tries to accommodate all objects hosting an AGN within the same scenario, is not able to explain the characteristics of some

Table 1: Sample of galaxies and results of the analysis.

Name (1)	Optical class. (2)	X-ray class. (3)	Variability		
			Analysis (var. par.) (4)	Flux (X-rays) (5)	Flux (UV) (6)
NGC 315	L1.9	AGN	SMF0	0 %	No data
NGC 1052	L1.9	AGN	SMF2 ($Norm_2, N_{H2}$)	20 %	21 %
NGC 1961	L2	AGN	SMF0	0 %	No data
NGC 2681	L1.9	AGN	SMF0	0 %	No data
NGC 2787	L1.9	AGN	-	-	No data
NGC 2841	L2	AGN	-	-	No data
NGC 3226	L1.9	AGN	-	-	11 %
NGC 3608	L2/S2:	Non-AGN	SMF0	0 %	No data
NGC 3718	L1.9	AGN	SMF1($Norm_2$)	29 %	No data
NGC 4261	L2	AGN	SMF0	0 %	34 %
NGC 4278	L1.9	AGN	SMF1($Norm_2$)	29 %	No data
NGC 4374	L2	AGN	SMF1($Norm_2$)	71 %	No data
NGC 4494	L2::	AGN	SMF1($Norm_2$)	35 %	No data
NGC 4636	L1.9	Non-AGN	SMF0	0 %	28 %
NGC 4736	L2	AGN	SMF0	0 %	66 %
NGC 5195	L2:	AGN	SMF1($Norm_2$)	20 %	16 %
NGC 5813	L2:	Non-AGN	SMF0	0 %	8 %
NGC 5982	L2::	AGN	SMF1($Norm_2$)	49 %	0 %

of them. For example those of low ionization nuclear emission line region nuclei (LINER), that were first classified in the optical using diagnostic diagrams [4].

At hard X-ray energies, where the AGN is more accesible, LINERs can be divided into AGN candidates when a point-like source is detected, or non-AGN candidates otherwise [1]. The most extensive work on this subject showed that $\sim 60\%$ of the LINERs in their sample are AGN candidates [1].

One of the main properties characterizing AGN is their variability at different wavelengths. For LINERs, the first clear evidence was reported at UV frequencies [8] and later some studies have been performed at X-rays, concluding that variability is common among them [10, 12, 2, 5]. However, the mechanism responsible of these variations is still not known. Using X-ray binaries (XRB) and AGN with good measurements of the black hole masses, bolometric luminosities, and variability timescales, T_B ¹, a variability plane has been defined, linking objects spanning a wide range of BH masses [9, 3].

Our aim is to study the main driver of the X-ray variability in LINERs; including how these measurements fit in the variability plane.

2 Sample and data reduction

We used the Palomar sample [7], which is the largest sample of nearby galaxies with optical spectra, containing HII nuclei, Seyferts, LINERs, and transition objects. We made use of all the publicly available *XMM*–Newton and *Chandra* data in more than one epoch for each

¹This T_B or bend timescale corresponds to a characteristic frequency, ν_B , of the power spectral density (PSD), which occurs when the spectral index of the power law bends from ~ 1 to ~ 2 .

object up to October 2013. The final sample of LINERs contains 18 objects, 8 of type 1, 10 of type 2, 15 AGN candidates and 3 non-AGN candidates². Table 1 shows both optical and X-ray nuclear classifications (Col. 2 and 3).

Chandra and *XMM*–Newton data were reduced in a systematic, uniform way using standard software analysis packages. Details on the sample selection and reduction can be found in [6].

3 Methodology

The detailed methodology can be found in [5, 6]. *XSPEC*³ version 12.7.0 was used for the spectral fitting. We summarize it in the following.

Individual spectral analysis: We first selected the best fit model for each data set individually. Five different models were used to fit the data; a thermal model (MEKAL in *XSPEC*, ME), a power law model (PL) or a composite model using these two simple models (2PL, MEPL, and ME2PL). The $\chi^2/d.o.f$ and F-test were used to select the simplest model that best represents the data.

Simultaneous spectral analysis: We simultaneously fitted the spectra for each object with the same model, which was selected from the individual fittings. For each galaxy, the initial values for the parameters were set to those obtained for the spectrum with the largest number counts. The simultaneous fit was made in three steps:

0. SMF0 (Simultaneous fit 0): The same model was used with all parameters linked to the same value to fit every spectra of the same object, i.e., this represents non-variable sources.
1. SMF1: Using SMF0 as the baseline for this step, we let one parameter (N_{H1} , N_{H2} , Γ , $Norm_1$, $Norm_2$, and kT) vary individually. The best fit was selected as that with the χ_r^2 closest to unity that improved SMF0 (using the F-test). This represents when only one parameter is needed to explain variations.
2. SMF2: Using SMF1 as the baseline for this step (when SMF1 did not fit the data well), we let two parameters vary, the one that varied in SMF1 along with any of the other parameters of the fit. The χ_r^2 and F-test were again used to confirm any improvement of the fit.

An example of the simultaneous fitting for NGC 5195 is shown in Fig. 1, where five spectra were fitted with the MEPL; the best-fit used SMF1 with the normalization of the power law, $Norm_2$, as the parameter varying.

Flux variability: X-ray luminosities were calculated from the best-fit models. UV data from the OM onboard *XMM*–Newton were used when available (simultaneously with X-ray data). In both cases, we assumed an object to be variable when $L_{max} - L_{min} > 3 \times \sqrt{(err(L_{max}))^2 + (err(L_{min}))^2}$.

²The objects were divided in AGN candidates and non-AGN candidates as in [1].

³<http://heasarc.nasa.gov/xanadu/xspec/>

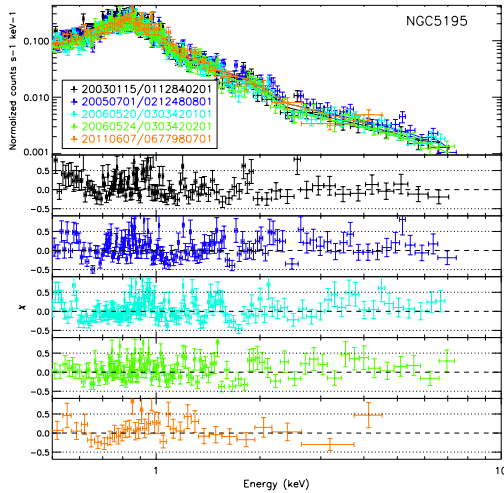


Figure 1: Example of the simultaneous fitting from the NGC 5195 spectra in five epochs with *XMM*–Newton data using the MEPL model. The best fit results in $Norm_2$ as the variable parameter (SMF1 was used). The legend shows the date (yyyymmdd) and the obsID. The residuals are shown from the second row on.

Short timescale variability: We calculated the normalized excess variance, σ_{NXS}^2 , for each light curve segment with 30–40 ksec following prescriptions in [11].

4 Results and discussion

The main results of this study are summarized in Table 1 (Cols. 4 to 6). Short term variations are not found. We find that all the objects that show long term X-ray spectral variations also show flux variability; none of the three non-AGN candidates (one type 1 and two type 2) show variations, while seven out of the 12 AGN candidates (three out of five type 1, and four out of seven type 2) do show variability (boldfaced in Col. 5 of Table 1). The X-ray analysis cannot be performed in three cases because the extended emission cannot be decontaminated. In one case (NGC 1052, type 1) SMF2 was used, with variations in the column density (N_{H2}) and the normalization of the power law ($Norm_2$). In all the variable cases $Norm_2$ is responsible for the observed variations (between 20–73%). Variations were found irrespective of the optical classifications.

Data at UV frequencies were available in eight out of the 18 cases. Variable objects are boldfaced in Col. 6 of Table 1; two of them are non-AGN candidates, and five are AGN candidates.

In summary, taking into account long term UV and/or X-ray variations, ten out of the 13 AGN candidates are variable (boldfaced in Col. 1 of Table 1); four out of six are type 1, and six out of seven are type 2. We note that the three objects without variations at X-ray frequencies (NGC 315, NGC 2681, and NGC 1961) do not have UV data in more than one

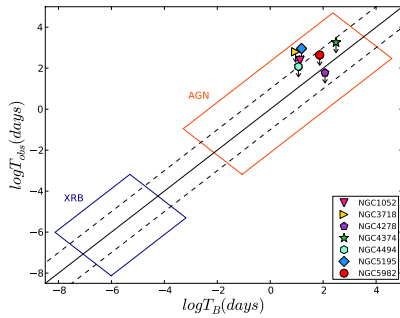


Figure 2: Observed variability timescale, T_{obs} , against the predicted value, T_B . The solid line represents the 1:1 relationship, the dashed lines the errors. Only variable objects are represented. Rectangles show the location of AGN (orange) and XRB (blue) as in [9].

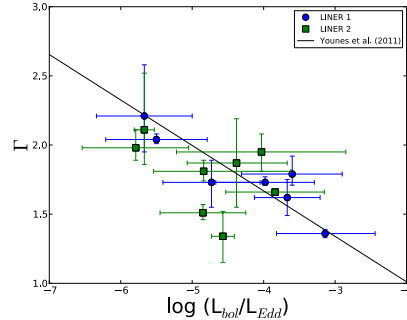


Figure 3: Anticorrelation between the slope of the power law, Γ , and the Eddington ratio. The solid line represents the relation given by [12].

epoch, so we cannot discard their variable nature. We notice that X-ray and UV variations did not happen simultaneously; the most natural explanation is the existence of time lags due to the time that light takes to travel in a disc-corona system.

These results show that the AGN continuum is changing with time. These kind of variations in other AGN follow the variability plane (see introduction, and also [9, 3]). Using the shortest periods in which variations were observed as upper limits of the observed variability timescales, T_{obs} , we plotted T_{obs} against T_B for the sources with variations in our sample in Fig. 2. We also plotted the location of AGN (big orange rectangle) and XRB (small blue rectangle) as reported in [9]. It can be observed that LINERs are located in the upper part of the relation together with the most massive AGN. This is most probably due to the strong dependence of T_B on the M_{BH} [9, 3].

However, it has been suggested that the accretion mechanism in LINERs may be different to that happening in more powerful AGN, and advection dominated accretion flows (ADAF) can play a role [12]. An indication of this behaviour would be an anticorrelation between the slope of the power law, Γ , and the Eddington ratio, L_{Edd} . The position of our objects in this correlation (see Fig. 3) suggests that ADAF may apply to LINERs.

5 Conclusions

Using *Chandra* and *XMM-Newton* public archives, we performed an analysis of both spectral and flux variability at short and long timescales of 18 LINERs in the Palomar sample. We found that seven out of the 12 AGN candidate LINERs show long-term spectral variability, while the three non-AGN candidates do not. There was no significant difference in the

proportion of X-ray variable nuclei among type 1 or 2. UV flux variations were found in five out of six AGN candidates, and in two non-AGN candidates. However, short-term variations were not found. In summary, considering both X-ray and UV data, we find that ten out of 13 LINERs in our sample show evidence of long-term variability in at least one energy band.

X-ray variations are caused by changes in the continuum of the AGN (the main driver of the spectral variations is the change in the normalization of the power law, N_{norm_2} ; only for NGC 1052 is this accompanied by variations in the column density, N_{H_2}). These results agree well with the expected variations according to their BH masses and accretion rates. In this sense, LINERs occupy the same locus as more powerful AGN and XRB. However, we find an anticorrelation between the slope of the power law and the Eddington ratio, what may suggest a different accretion mechanism in LINERs.

Acknowledgments

This work was financed by MINECO grant AYA 2010-15169, AYA 2012-39168-C03-01, AYA 2013-42227-P, Junta de Andalucía TIC114 and Proyecto de Excelencia de la Junta de Andalucía P08-TIC-03531. This research made use of data obtained from the *Chandra* Data Archive provided by the *Chandra* X-ray Center (CXC), and from from the *XMM-Newton* Data Archive provided by the *XMM-Newton* Science Archive (XSA).

References

- [1] González-Martín, O., Masegosa, J., Márquez, I., Guainazzi, M., & Jiménez-Bailón, E. 2009, *A&A*, 506, 1107
- [2] González-Martín, O., Papadakis, I., Braitto, V., Masegosa, J., Márquez, I., Mateos, S., Acosta-Pulido, J. A., Martínez, M. A., Ebrero, J., Esquej, P., O'Brien, P., Tueller, J., Warwick, R. S., Watson, & M. G. 2011, *A&A*, 527, A142
- [3] González-Martín, O., & Vaughan, S. 2012, 544, A80
- [4] Heckman, T.M. 1980, *A&A*, 87, 152
- [5] Hernández-García, L., González-Martín, O., Márquez, I., & Masegosa, J. 2013, *A&*, 556, A47
- [6] Hernández-García, L., González-Martín, O., Masegosa, J. & Márquez, I. 2014, 569, A26
- [7] Ho, L. C., Filippenko, A. V., Sargent, W. L. W., & Peng, C. Y. 1997, *ApJS*, 112, 391
- [8] Maoz, D., Nagar, N. M., Falcke, H., & Wilson, A. S. 2005, *ApJ*, 625, 699
- [9] McHardy, I. M., Koerding, E., Knigge, C., Uttley, P. & Fender, R. P. 2006, *Nature*, 444, 730
- [10] Pian, E., Romano, P., Maoz, D., Cucchiara, A., Pagani, C., & Parola, V. L. 2010, *MNRAS*, 401, 677
- [11] Vaughan, S., Edelson, R., Warwick, R. S. & Uttley, P. 2003, *MNRAS*, 345, 1271
- [12] Younes, G., Porquet, D., Sabra, B., & Reeves, J. N. 2011, *A&A*, 530, A149